Physicochemical and Biochemical Properties of 2′,5′-Linked RNA and 2′,5′-RNA:3′,5′-RNA "Hybrid" Duplexes[†,‡]

Marita Wasner,[§,||] Dominique Arion,[⊥] Gadi Borkow,[⊥,▽] Anne Noronha,[§] Andre H. Uddin,[§,⊗] Michael A. Parniak,[⊥] and Masad J. Damha*[,§]

Department of Chemistry, McGill University, Montreal, Quebec, Canada H3A 2K6, and McGill AIDS Center and Faculty of Medicine, McGill University, Montreal, Quebec, Canada H3T 1E2

Received January 21, 1998; Revised Manuscript Received March 9, 1998

ABSTRACT: In recent publications, oligonucleotides joined by 2′,5′-linkages were found to bind to complementary single-stranded RNA but to bind weakly, or not at all, to single-stranded DNA [e.g., P. A. Giannaris and M. J. Damha (1993) *Nucleic Acids Res. 21*, 4742−4749]. In this work, the biochemical and physicochemical properties of 2′,5′-linked oligoribonucleotides containing mixed sequences of the four nucleobases (A, G, C, and U) were evaluated. CD spectra of RNA:2′,5′-RNA duplexes were compared with the spectra of DNA:DNA, RNA:RNA, and DNA:RNA duplexes of the same base sequence. The CD results indicated that the RNA:2′,5′-RNA duplex structure more closely resembles the structure of the RNA:DNA hybrid, being more A-form than B-form in character. The melting temperature (T_m) values of the backbone-modified duplexes were compared with the T_m values of the unmodified duplexes. The order of thermal stability was RNA:RNA > DNA:DNA ≈ RNA:DNA ≈ DNA:RNA > RNA:2′,5′-RNA > 2′,5′-RNA:2′,5′-RNA ≫ DNA:2′,5′-RNA (undetected). RNA:2′,5′-RNA duplexes are not substrates of the enzyme RNase H (*Escherichia coli*, or HIV-1 reverse transcriptase), but they can inhibit the RNase H-mediated cleavage of a natural DNA:RNA substrate. Structural models that are consistent with the selective association properties of 2′,5′-linked oligonucleotides are discussed.

The ability of modified oligonucleotides to form a duplex with a particular RNA[1] species enables specific control of gene expression ("antisense strategy") (*1*). Our earlier work on the hybridization properties of oligoribonucleotides constructed of 2′,5′-internucleotide linkages, i.e., 2′,5′-(rPy)$_n$rPy and 2′,5′-(rA)$_n$rA, proved that these molecules hybridize to complementary RNA strands, but they hybridize weakly or not at all to complementary single-stranded DNA strands (*2, 3*). For example, in a solution of 0.1 M NaCl and 0.01 M phosphate buffer (pH 7.0), the tridecamer 2′,5′-r(CCC UCU CCC UUC U) will form a duplex with its Watson−Crick RNA complement with a single transition temperature of about 40 °C as measured by ultraviolet absorbance. Under identical conditions, however, no complex formation between this 2′,5′-oligomer and its complementary DNA strand could be observed (*3*). In addition, we found that substituting a few 3′,5′-linkages with the 2′,5′-linkage within r(Ap)$_9$A destabilized binding to poly-dT (−4.2 °C/2′,5′-linkage) more so than to poly-rU (−1.3 °C/linkage) (*2, 3*). Since our first reports in 1991 (*2*) and 1993 (*3*), other 2′,5′ -oligonucleotide analogues have been shown to display similar association behavior, namely, single-stranded 2′,5′-linked DNA (*4*−*7*), 2′,5′-linked thioformacetal ssDNA (*8*), and 2′,5′-ribo/3′,5′-deoxyribonucleotide chimeras (*9*), suggesting that this may represent a general feature of oligomers constructed with 2′,5′-internucleotide linkages (Figure 1).

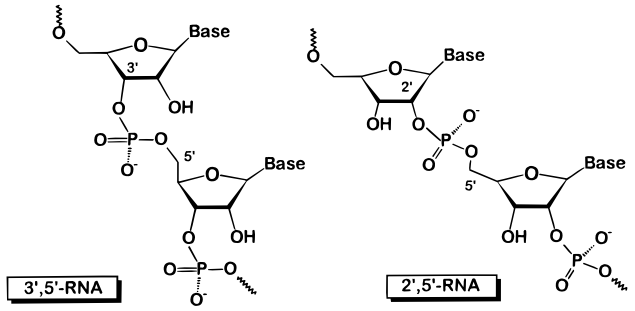

FIGURE 1: Structures of single-stranded 3′,5′-RNA and 2′,5′-RNA.

The potential benefits of 2′,5′-linked oligonucleotides as antisense therapeutics are clearly evident from recent studies

[†] This research was supported by a Strategic Grant (STR-181477) to M.J.D. and M.A.P. from the National Sciences and Engineering Research Council of Canada (NSERC) and by a grant by BioChem Therapeutics, Inc. (BioChem Pharma) to M.J.D. M.A.P. is an International Research Scholar of the Howard Hughes Medical Institute.

[‡] Dedicated to Prof. Fritz Eckstein on the ocassion of his 65th birthday.

* To whom correspondence should be addressed: Otto Maass Chemistry Building, 801 Sherbrooke St. W., Montreal, Quebec, Canada H3A 2K6. Telephone: (514) 398-7552. Fax: (514) 398-3797. E-mail: damha@omc.lan.mcgill.ca.

[§] Department of Chemistry.

[||] Current address: Cyanamid Forschung GmbH, P.O. Box 100, Zur Propstei, D-55270 Schwabenheim, Germany.

[⊥] McGill AIDS Center and Faculty of Medicine.

[▽] Current address: R. Ben-Ari Institute of Clinical Immunology, AIDS Center, Kaplan Medical Center, Rehovot 76100, Israel.

[⊗] Current address: Midlan Walwyn Capital, 181 Bay Street, Suite 500, Toronto, Ontario, Canada M5J 2V8.

[1] Abbreviations: AON, antisense oligonucleotide; CD, circular dichroism; DNA, single-stranded 3′,5′-linked deoxyribonucleic acid; 2′,5′-DNA, single-stranded 2′,5′-linked deoxyribonucleic acid; RNA, 3′,5′-linked ribonucleic acid; 2′,5′-RNA, 2′,5′-linked ribonucleic acid; RNase H, ribonuclease H enzyme; RT, reverse transcriptase enzyme.

S0006-2960(98)00160-3 CCC: $15.00
Published on Web 05/02/1998

described in the literature (*7, 9, 10*). For instance, single-stranded 2′,5′-/3′,5′-DNA phosphorothioate or phosphate chimeras resist enzymatic hydrolysis and have been shown to inhibit steroid 5α-reductase expression in cell cultures (*7*). There is also evidence that single-stranded DNA/2′,5′-RNA chimeras and 2′,5′-DNA show less nonspecific binding to plasma and cellular proteins in comparison with 3′,5′-phosphorothioate (PS) oligodeoxynucleotides (*7, 9*), a property that may produce fewer side-effects in vivo. Furthermore, studies employing antisense DNA/2′,5′-rA_n chimeras indicate that the 2′,5′-rA_n portion of these oligomers directs cleavage of targeted RNA, presumably through activation of RNase L in cell culture (*10*).

To get insight into the unusual RNA binding selectivity of 2′,5′-RNA and the properties of RNA:2′,5′-RNA "hybrid" duplexes, we decided to prepare 2′,5′-oligoribonucleotides containing mixed sequences of all four nucleobases. Specifically, we carried out an analysis of the conformation of RNA: 2′,5′-RNA hybrid duplexes using circular dichroic spectroscopy (CD) and molecular modeling. We have also assessed the susceptibility of these duplexes to hydrolysis by the enzymes RNase H (*Escherichia coli* and HIV-1 reverse transcriptase). Finally, we discuss possible structural models that are consistent with the selective association properties of 2′,5′-linked oligonucleotides and available data in the literature.

MATERIALS AND METHODS

Materials. Recombinant heteropolymeric p51/p66 HIV-1 RT was purified from lysates of *E. coli* JM-105 transformed with expression plasmids pRT66 and pRT51 (*11*) using a rapid single-step purification method we have recently described (*12, 13*). *E. coli* RNase H was obtained from Pharmacia. 5′-*O*-Dimethoxytrityl 2′-*O*-*tert*-butyldimethylsilylribonucleoside 3′-*O*-phosphoramidite monomers for normal RNA synthesis were obtained from Dalton Chemical Laboratories, Inc. (Ontario, Canada). The corresponding ribonucleoside 2′-*O*-phosphoramidites were either synthesized by modifications of published procedures (*14, 15*) or obtained commercially from ChemGenes Corp. (Waltham, MA).

2′,5′- and 3′,5′-Oligoribonucleotide Synthesis. Syntheses were carried out on an Applied Biosystems DNA/RNA 381A synthesizer. Oligomers were prepared on a 1μmol scale using 1,12-diaminododecyl controlled pore glass (500 Å) (*16*) derivatized with 5′-DMT-N^4-benzoyl-2′-*tert*-butyldimethylsilylcytidine. Ribonucleoside 2′-(or 3′-)phosphoramidites were dissolved to 0.12−0.17 M in anhydrous acetonitrile. Best results were obtained when 5-ethylthio-1*H*-tetrazole (0.65 M in acetonitrile) was used as the coupling catalyst (*17, 18*). When 1*H*-tetrazole was used instead, 2′-amidite monomers coupled with only ∼85−95% efficiency on the basis of dimethoxytrityl color analysis. Prior to chain assembly, the support was treated with the capping reagents acetic anhydride/*N*-methylimidazole/DMAP, as previously described (*15*). Assembly of 2′,5′-RNA sequences was carried out as described (*3, 15*) with the following changes: (a) Detritylation: 3% trichloroacetic acid in dichloroethane delivered in 100-s (+ 40-s burst) steps. The eluate from this step was collected, and the absorbance at 504 nm was measured to determine condensation yields. (b) Phosphoramidite coupling: coupling time, 7.5 min. (c) Capping: acetic anhydride/collidine/THF, 1:1:8 (solution A), and 1-methyl-1*H*-imidazole/THF, 16:84 (solution B), delivered in 62-s + 35-s wait steps. (d) Oxidation: 0.05 M iodine in THF/water/pyridine, 7:2:1, delivered in 20-s + 35-s wait steps. These conditions gave ∼98.8% average condensation yields for the 2′,5′-linked sequences, with purine momers coupling better (∼99.7%) than pyrimidine monomers (∼97.1%). Similar results were obtained for the synthesis of the corresponding 3′,5′-linked RNA sequences.

Following chain assembly, the CPG support was taken out of the column and divided into two portions (0.5 μmol each). Each portion was treated with aqueous ammonia/ethanol (3:1, v/v, 1.2 mL) for 2 days at room temperature. After centrifugation, the supernatant was collected and the support was washed with EtOH. The supernatant and ethanol washings were evaporated, and the pellet obtained was treated with neat NEt_3·3 HF (60 μL) at room temperature for 36 h (*19*). The oligomers were precipitated by adding 4 M aqueous sodium acetate (25 μL) and butanol (1 mL) and cooling the resulting solutions to −20 °C for at least 2 h. The supernatant was removed following centrifugation, and the pellets (oligomers) were washed with cold 70% EtOH (2 × 300 μL) and dried.

Sequences were purified by anion-exchange HPLC on a Protein Pak DEAE-5PW 7.5 × 75 mm (Waters) column using a gradient of 0−20% aqueous 1M $NaClO_4$ over 40 min with detection at 280 nm. Alternatively, oligomers were purified by preparative polyacrylamide gel electrophoresis (PAGE) followed by gel filtration (desalting) on a Sephadex G-25 column (*15*). Isolated yields (HPLC): 30−50 A_{260} units (∼1−2 mg). The structures were confirmed by MALDI-TOF mass spectrometry.

Molecular Modeling Experiments. A-form RNA:RNA (C3′-endo) and B-form DNA:DNA (C2′-endo) duplex structures were generated using HyperCube's molecular modeling system (HyperChem, version 5.0). The RNA:2′,5′-RNA duplex structure was constructed from the RNA:RNA duplex by replacing the 3′,5′-linkages in one of the RNA strand with 2′,5′-linkages. The 3′,5′ to 2′,5′ substitutions were carried out one at a time, starting from the 3′-end of the strand and minimizing the duplex after each substitution. Similarly, the DNA:2′,5′-RNA duplex was constructed from the energy-minimized DNA:RNA duplex. The AMBER force field (switching function between 10 and 14 Å) was applied for energy minimizations on unconstrained helices, and no counterions were included. When possible, molecular dynamic simulations was performed at 300 K with a step size of 1.0 fs for a period of 15 ps using a distance-dependent dielectric constant of 4*r*. This was followed by another minimization procedure. Stereoviews of energetically favored structures are shown in Figure 4.

UV Thermal Denaturation Studies. UV thermal denaturation data was obtained on a Varian CARY 1 spectrophotometer equipped with a Peltier temperature controller. Molar extinction coefficients for DNA and RNA strands were estimated using the nearest-neighbor approximation (*20*). Molar extinction coefficients for 2′,5′-linked RNA were assumed to be the same as those of normal RNA strands, and are as follows (in 10^4 M^{-1} cm^{-1} units): 2′,5′-(R)RNA, 17.52; 2′,5′-(U5)RNA, 24.03; 2′,5′-sense(U5)-RNA, 22.97. Oligomers were mixed in equimolar ratios in 140 mM K^+,

Table 1: Melting Temperature (T_m) Values of Duplexes of DNA, RNA, and 2′,5′-RNA Oligomers with Complementary Target DNA and RNA Strands

designation	oligonucleotide	T_m (°C)[a] complementary 3′,5′- ssDNA	RNA
R region			
3′,5′-(R)DNA	5′-dAGC TCC CAG GCT CAG ATC-3′	68.5	72.3
3′,5′-(R)RNA	5′-rAGC UCC CAG GCU CAG AUC-3′	66.7	84.6
2′,5′-(R)RNA	5′-rAGC UCC CAG GCU CAG AUC-2′	*b*	64.4
U5 region			
3′,5′-(U5)DNA	5′-dGT CTG TTG TGT GAC TCT GGT AAC-3′	67.0	65.0
3′,5′-(U5) RNA	5′-rGU CUG UUG UGU GAC UCU CCU AAC-3′	67.0	79.0
2′,5′-(U5)RNA	5′-rGU CUG UUG UGU GAC UCU CCU AAC-2′	*b*	56.5
		complementary 2′,5′-RNA, T_m (°C)[a]	
2′,5′-(U5)RNA	5′-rGU CUG UUG UGU GAC UCU CCU AAC-2′	41.1	

[a] Buffer: 140 mM K^+, 1 mM Mg^{2+}, and 5 mM Na_2HPO_4, pH 7.2; see Materials and Methods for experimental details. [b] Broad transition with small hyperchromicity that derives from melting (unstacking) of the 2′,5′-ssRNA.

1 mM Mg^{2+}, and 5 mM Na_2HPO_4 buffer, pH 7.2 (*21*). The total strand concentration was 5.5 μM. Samples were heated to 80 °C for 5 min, cooled slowly to room temperature, and refrigerated (5 °C) overnight before measurements. Prior to the thermal run, samples were degassed by placing them in an ultrasound bath or under vacuum (Speed-Vac concentrator) for 2 min. Denaturation curves were acquired at 260 nm at a rate of heating of 0.5 °C/min. The data were analyzed with the software provided by Varian Canada and transferred to Microsoft Excel for presentation. Melting temperatures (T_m) were calculated from first-derivative plots of absorbance versus temperature.

Circular Dichroism (CD) Spectra. Spectra (200−350 nm) were collected on a Jasco J-710 spectropolarimeter at a rate of 100 nm/min using fused quartz cells (Hellma, 165-QS). Measurements were carried out in 140 mM K^+, 1 mM Mg^{2+}, and 5 mM Na_2HPO_4 buffer, pH 7.2, at a duplex concentration of 5.5 μM. Temperature was controlled by an external constant temperature NESLAB RTE-111 circulating bath. The data were processed on a PC computer using Windows-based software supplied by the manufacturer (JASCO, Inc.). To facilitate comparisons, molar ellipticities were calculated from the known nucleotide concentrations and the spectra obtained.

RNase H Induction Assays. In vitro RNase H assays measured the degradation of 3′,5′-(R)senseRNA (18 nt) and 3′,5′-(U5)sense RNA (23 nt) (Table 1), corresponding respectively to a sequence within the R and U5 regions of HIV-1_{3b} genomic RNA. RNase H assays were carried out in a total volume of 10 μL which comprised 2.5 pmol of the 5′-^{32}P-end-labeled RNA, 7.5 pmol of an oligonucleotide (DNA, RNA, or 2′,5′-RNA) of the same length and exactly complementary to the ^{32}P-end-labeled RNA, 60 mM Tris-HCl, 2 mM dithiothreitol, 60 mM KCl, and either 2.5 mM $MgCl_2$ or 0.1 mM $MnCl_2$ as metal activators (pH 7.8). Reactions were initiated by the addition of HIV-1 RT (0.2 pmol of p51/p66 heterodimer) or *E. coli* RNase H (0.4 unit) and then allowed to proceed for varying times at 37 °C. Reactions were quenched with loading buffer (98% deionized formamide, 10 mM EDTA, 1 mg/mL bromophenol blue, and 1 mg/mL xylene cyanol) followed by incubation at 100 °C for at least 5 min. The reaction mixtures containing normal RNA duplex (R region) were difficult to denature, requiring at least 20 min at 100 °C prior to electrophoresis (T_m = 85 °C). Reaction products were resolved on a 16% sequencing polyacrylamide gel containing 7 M urea in 45 mM Tris-borate/1 mM EDTA (pH 8) and visualized by autoradiography.

Duplex Competition RNase H Binding Experiments. These experiments measured the ability of various duplexes to inhibit the RNase H-mediated degradation of a 5′-^{32}P-labeled RNA:DNA 23-bp duplex substrate. The base sequence of the labeled RNA strand of this substrate was 5′-CAG ACA ACA CAC UGA GAC CAU UG-3′ [3′,5′-(U5)sense RNA; Table 1], which corresponds to a sequence within the U5 region of HIV-1_{3B} genomic RNA. The competitor duplexes were preformed by incubating unlabeled 3′,5′-(U5)sense RNA with an equimolar amount of complementary sequence 23-nt oligonucleotide (DNA, RNA, or 2′,5′-RNA) at 70 °C for 3 min, followed by slow cooling to room temperature over a 1-h period. The competitor duplex (2.5 pmol) was added to RNase H reaction assays (10 μL total volume) comprised of 1 pmol of 5′-^{32}P-labeled RNA:DNA duplex substrate in 60 mM Tris-HCl (pH 7.8, 37 °C) containing 60 mM KCl, 2 mM dithiothreitol, and either 10 mM $MgCl_2$ or 0.1 mM $MnCl_2$. Reactions were initiated by the addition of HIV-1 RT (0.06 pmol of p51/p66 heterodimer) or *E. coli* RNase H (0.04 unit) and then allowed to proceed for varying times at 37 °C. Reactions were quenched by the addition of 10 μL of a solution consisting of 98% deionized formamide, 10 mM EDTA, 1 mg/mL bromophenol blue, and 1 mg/mL xylene cyanol, followed by incubation at 100 °C for at least 5 min. Reaction products were visualized by autoradiography after electrophoretic resolution on 16% sequencing polyacrylamide gels containing 7 M urea in 45 mM Tris-borate/1 mM EDTA (pH 8).

RESULTS AND DISCUSSION

Design and Synthesis of 2′,5′-Linked Oligoribonucleotides. The RNA hybridization selectivity of oligonucleotides constructed from 2′,5′-internucleotide linkages was first characterized in our laboratory in the ribo series (*2*, *3*). Further studies in the deoxy series were carried out by others (*4*−*8*), who demonstrated that 2′,5′-DNA strands and their analogues possessed the same hybridization selectivity. Thus far, no systematic investigations of RNA:2′,5′-RNA duplexes have been reported, except for our previous reports which were restricted to the association of 2′,5′-linked oligoriboadenylates and oligoribopyrimidines with RNA and DNA strands (*2*, *3*). In this study, we prepared 2′,5′-RNA oligomers containing the four nucleobases, as they are more ideal models for hybridization studies and biological investigations.

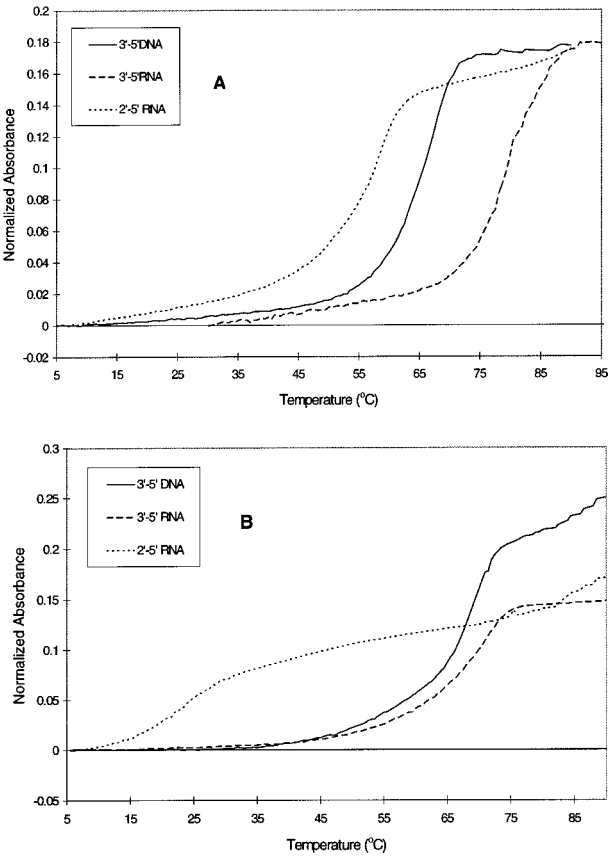

FIGURE 2: Thermal melting curves of 23-bp U5 region duplexes. Oligonucleotides were hybridized to (A) single-stranded 3′,5′-linked RNA and (B) 3′,5′-linked DNA. See Table 1 for base sequence (U5 region). Buffer: 140 mM K^+, 1 mM Mg^{2+}, and 5 mM Na_2HPO_4, pH 7.2. See Materials and Methods for experimental conditions.

A 2′,5′-linked octadecanucleotide and a 2′,5′-linked tricosanucleotide were prepared and designed to be complementary to the R and U5 regions, respectively, of genomic HIV-1 RNA (Table 1). To investigate the potential formation of a pure 2′,5′-RNA:2′,5′-RNA duplex, we also prepared the Watson−Crick complement of the tricosanucleotide sequence. As controls, we also synthesized the natural RNA and ssDNA strands of the same sequences, along with their complementary RNA and ssDNA strands. Sequences of the oligonucleotides prepared for this study are indicated in Table 1.

UV Thermal Melting Study: Selective RNA Recognition by 2′,5′-RNA. Melting curves of 2′,5′-oligomers annealed to complementary RNA and single-stranded DNA were obtained in a buffer containing 140 mM K^+, 1 mM Mg^{2+}, and 5 mM Na_2HPO_4 (pH 7.2), which is representative of intracellular conditions (*21*). Thermal dissociation (T_m) data for the complexes formed are summarized in Table 1.

The 23-bp duplex of 2′,5′-(U5)RNA with RNA showed a single cooperative transition at 56.5 °C, while an equimolar mixture of 2′,5′-(U5)RNA and DNA showed a much weaker and broader transition that is derived from the 2′,5′-strand alone (Figure 2; compare panels A and B). Analogous results were obtained for the R-region duplexes: the G/C-rich 18-bp RNA:2′,5′-RNA duplex displayed a cooperative transition centered at 64 °C (Table 1), whereas no complex was detected between 2′,5′-(R)RNA and its complementary DNA strand. Polyacrylamide gel electrophoresis (PAGE) shift assays were consistent with the conclusions drawn from the UV melting data (not shown) and confirmed our earlier findings that 2′,5′-linked oligoribonucleotides associate with RNA, but they associate only weakly, or not at all, with single-stranded DNA (*2, 3*).

For comparison, we also investigated the unmodified RNA and DNA duplexes, the hybrid duplexes RNA:DNA and DNA:RNA, and the pure 2′,5′-RNA duplex. The key observations are as follows: (a) The RNA:2′,5′-RNA hybrids are of lower thermal stability than the pure 3′,5′-linked RNA duplexes (ΔT_m > 20 °C), suggesting that annealing of two normal RNA strands is thermodynamically more favorable than annealing of a 2′,5′-RNA strand with a normal RNA strand. (b) The mutually complementary 2′,5′-RNA strands have the ability to associate, exhibiting a transition temperature that is considerably lower (T_m = 41 °C) than that of the corresponding 3′,5′-linked RNA duplex (T_m = 79 °C), and RNA:2′,5′-RNA duplex (T_m = 56.5 °C). This stability pattern, RNA duplex > 2′,5′-RNA duplex, has also been noted by Kierzek et al. (*24*) and by Giannaris and Damha (*3*) for shorter 2′,5′-oligoribonucleotide sequences, and it correlates with that observed for the deoxy molecules, i.e., DNA duplex > 2′,5′-DNA duplex (*25*−*27*). (c) A comparison of the T_m's of the *U5* duplexes revealed the following order of thermal stability: RNA:RNA > DNA:DNA ≈ RNA:DNA ≈ DNA:RNA > RNA:2′,5′-RNA > 2′,5′-RNA:2′,5′-RNA ≫ DNA:2′,5′-RNA (undetected) (Table 1).

Circular Dichroism (CD). (A) Unmodified Duplexes. With a few notable exceptions (*28, 29*), DNA duplexes have B-form structure in solution, whereas RNA duplexes are conformationally confined to the A-form (*28*). Natural DNA:RNA hybrids generally adopt a more complex sequence-dependent structure that is neither A nor B structure, but some intermediate or hybrid form between the A and B families (*30*−*33*). This is clearly exemplified by the CD spectra of the reference duplexes (U5 and R series) shown in Figure 3, panels B and C. The appearance of a strong positive band at ∼265 nm and a strong negative CD band near 210 nm in the spectrum of the normal RNA duplexes is characteristic of the A-conformation. On the other hand, the spectra of the DNA duplexes had positive and negative CD bands of moderate magnitudes at wavelengths above 220 nm and a crossover point at ∼260−265 nm typical of the B-DNA conformation. The CD spectra of the RNA:DNA hybrid duplexes displayed spectral features of the pure RNA and DNA duplexes with a greater similarity to the pure RNA spectra (Figure 3, panels B and C). For example, the negative band at 210 nm characteristic of the A-RNA conformation was much reduced in the spectra of the hybrids, and the positive ∼280−290-nm shoulder in the U5 hybrid coincided with the positive band of the B-DNA duplex (Figure 3B). These results are fully consistent with CD analysis of hybrids containing mixed purine−pyrimidine base composition (*30*−*33*).

(B) RNA:2′,5′-RNA and 2′,5′-RNA:2′,5′-RNA Duplexes. First, it is informative to compare the CD spectra of single-stranded 2′,5′-oligoribonucleotides with those of normal oligonucleotides. As shown in Figure 3A, the 2′,5′-linked (U5)RNA strand has much lower molar ellipticity values than the corresponding 3′,5′-linked (U5)RNA strand. This does not necessarily reflect reduced stacking in 2′,5′-RNA strands relative to normal RNA strands since the spectra of these

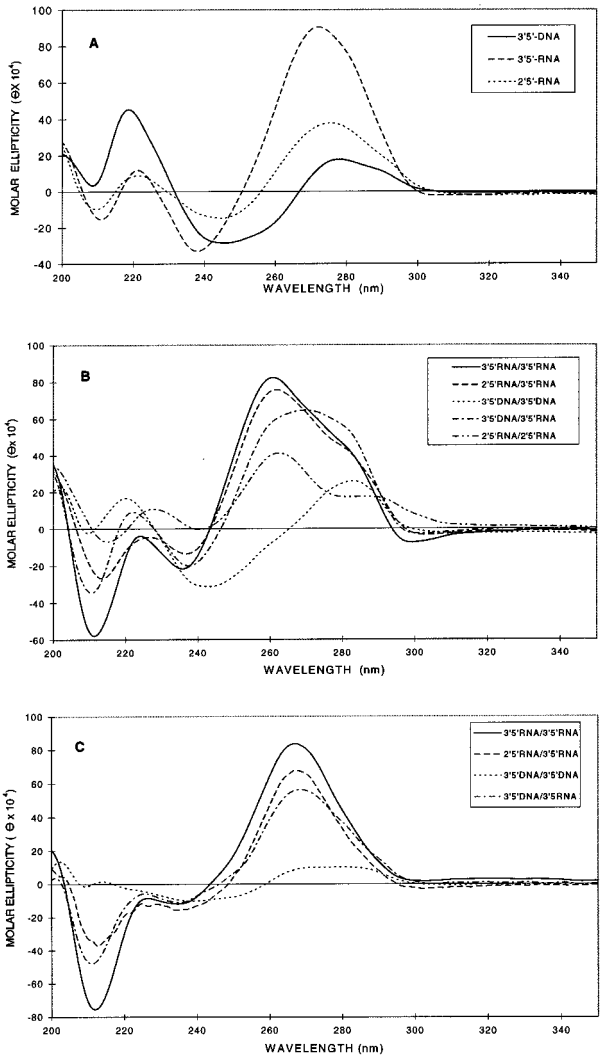

FIGURE 3: Circular dichroic (CD) spectra of (A) free single-strands, (B) 23-bp U5 region duplexes, and (C) 18-bp R region duplexes. Buffer: 140 mM K^+, 1 mM Mg^{2+}, and 5 mM Na_2HPO_4, pH 7.2. See Table 1 for base sequences and Materials and Methods for experimental conditions.

isomeric compounds have slightly different band positions (*36*, *37*). A more plausible explanation of the CD results is that the angle between the transition moments of the bases differs between the RNA strands and the 2′,5′-RNA strands, resulting in a smaller rotational strength for the 2′,5′-strand stacks relative to the 3′,5′-strand stacks (*36*, *37*). In fact, NMR and hypochromicity data indicate that the overlapping of the bases in single-stranded 2′,5′-RNA is more extensive than in single-stranded RNA (*36*−*41*).

As shown in Figure 3, panels B and C, the spectra of the RNA:2′,5′-RNA hybrids were more similar to those of the unmodified RNA duplexes than to those of the DNA duplexes; however, the negative band at 210 nm was reduced for RNA:2′,5′-RNA hybrids in comparison with the same band in the spectra of RNA duplexes. This showed that RNA:2′,5′-RNA hybrid duplexes adopt a global helical conformation of the A-family, with more A-form than B-form character. This property is shared with the unmodified RNA:DNA hybrids, whose CD patterns matched very well those of the corresponding RNA:2′,5′-RNA duplexes (Figure 3, panels B and C). In agreement with this conclusion, no unusual steric restriction was found in an energy-minimized molecular model of RNA:2′,5′-RNA in which a continuous A-type double-helical structure was maintained (Figure 4). However, the RNA:2′,5′-RNA helix had smaller interstrand phosphate−phosphate distances than those of the normal duplexes (by ca. 1 Å), which may account at least in part for the lower thermal stability of RNA:2′,5′-RNA relative to RNA:RNA and RNA:DNA helices (Table 2). Of interest, no remarkable structural change was observed in the 3′,5′-linked RNA strand that is common to the RNA:2′,5′-RNA, RNA:RNA, and RNA:DNA duplexes (Figure 4).

The CD spectra of a 1:1 mixture of 2′,5′-RNA and its complementary DNA strand did not differ significantly from the calculated average of the spectra of 2′,5′-RNA and DNA strands, confirming the lack of association of these strands (data not shown).

As shown is Figure 3B, the CD spectra of the pure 2′,5′-RNA homoduplex does not fall into a pure B-form or pure A-form pattern. The positive band at ca. 265 nm seems to resemble that of the pure 3′,5′-RNA, while the peak at ca. 290 nm and the 210−230 nm region resembles that of the pure DNA duplex. The conclusion from the CD data is that the spectra of the 2′,5′-RNA homoduplex is a mixture of the duplex DNA and RNA spectra, with less A-character than the RNA:DNA and RNA:2′,5′-RNA spectra.

Sugar Conformations of RNA:2′,5′-RNA and Normal Duplexes. Associated with the different structural forms of double helices are different sugar puckering modes, tilts of base pairs, and sizes of the minor and major grooves. A-form RNA duplexes are characterized by C3′-endo sugars and a wide and shallow minor groove, while the structure of B-form duplexes is characterized by C2′-endo sugars and a narrow and deep minor groove (*28*). NMR studies in solution have indicated a more complex structure for RNA:DNA hybrids, displaying C3′-endo sugar puckering for the RNA strand and C2′-endo/C4′-endo for the DNA strand (*34*, *35*). The similar CD spectra of RNA:2′,5′-RNA and RNA:DNA duplexes suggest the interesting possibility that the 2′,5′-RNA strand bears global structural similarity to the natural DNA strand. In agreement with this hypothesis, NMR studies of small 2′,5′-RNA molecules have shown that the sugars exist in a dynamic C2′−C3′-endo equilibrium, with a predominant C2′-endo pucker in many cases, e.g., the $rA^{2'p}$ residue in 2′,5′-ApU and 2′,5′-ApC (*40*, *41*). In addition, molecular modeling studies reported by Lalitha and Yathindra (*42*) have shown that a 2′,5′-RNA:2′,5′-RNA duplex with C2′-endo repeating nucleotides is stereochemically favored. With the C3′-endo sugar, the 3′-hydroxyl group sterically interferes with the phosphate linkages. In agreement with this result, the 2′,5′-RNA strand in the energy-minimized RNA:2′,5′-RNA duplex shown in Figures 4 and 5 takes predominantly the C2′-endo conformation, whereas the unmodified RNA strand takes the C3′-endo conformation. The C3′-endo pucker form of 2′,5′-RNA has been observed in crystal structures, e.g., in a 2′,5′-ApC:RNAse S complex (*43*), and in the unusual parallel-stranded miniduplex formed by 2′,5′-C^+pA in which both C2′- and C3′-endo forms coexist (*44*).

NMR investigations in solution demonstrate that oligomers of 3′-deoxynucleosides (e.g., 2′,5′-DNA) can also adopt C2′- and C3′-endo type conformations (*45*), although in most cases the C3′-endo sugar pucker predominates (*46*). This feature can be traced back to the properties of the monomeric

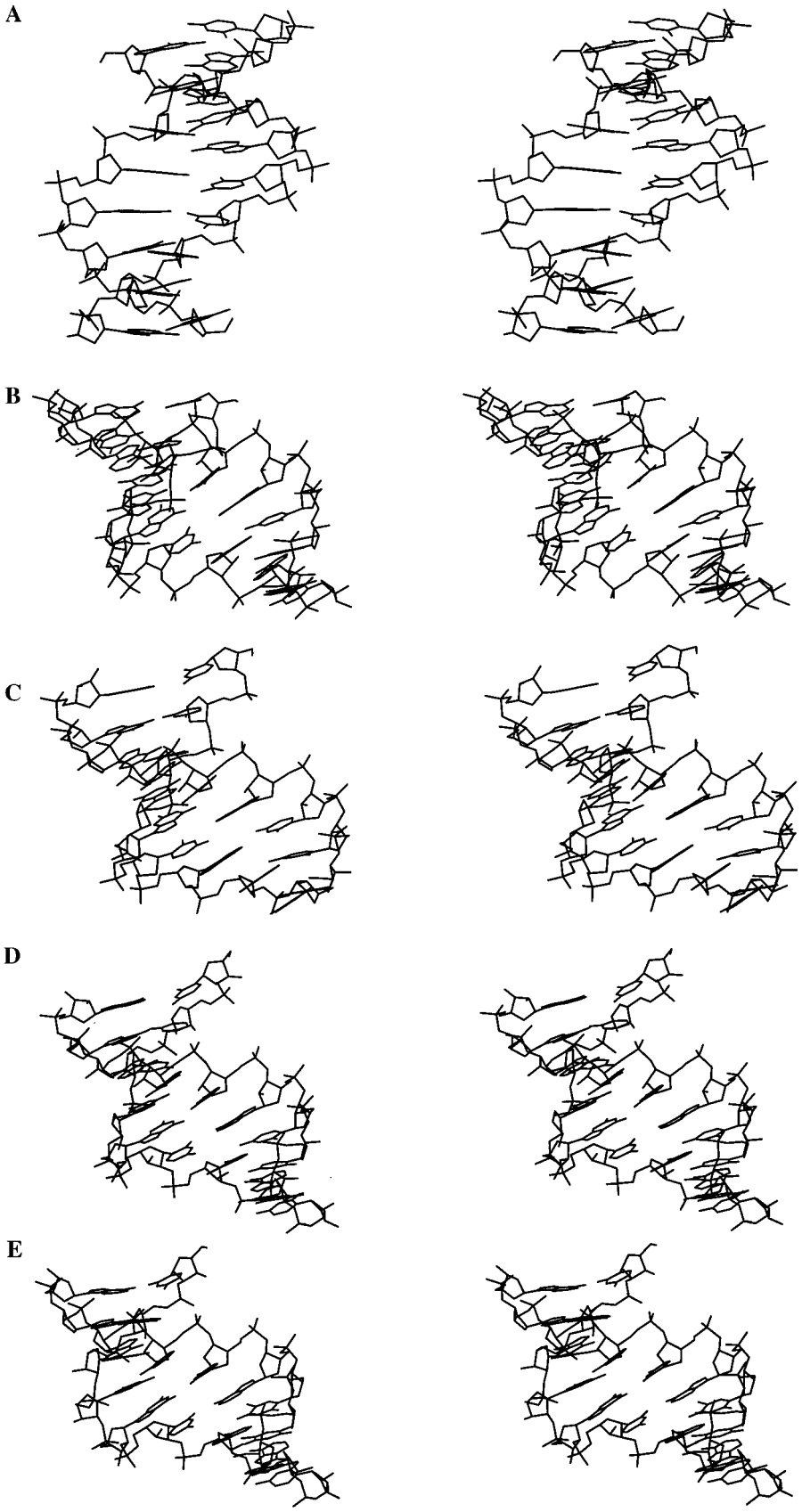

FIGURE 4: Stereo images of (A) the energy-minimized structure of a DNA:DNA 9-bp duplex compared to (B) RNA:RNA, (C) RNA:DNA, (D) RNA:2′,5′-RNA, and (E) 2′,5′-RNA:DNA duplexes. The common RNA strand of duplexes B, C, and D is shown at the top in each case. Properties of the minimized duplexes are given in Table 2.

3′-deoxynucleoside units, in which stereoelectronic effects stabilize the C3′-endo form (*46* and references therein).

Selectivity of 2′,5′-Oligonucleotides for RNA versus DNA Strands. It is an interesting endeavor to consider why 2′,5′-

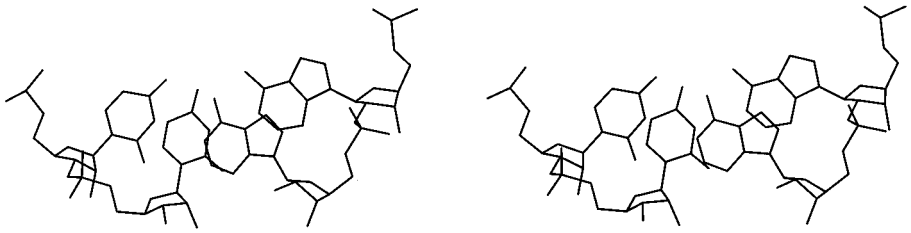

FIGURE 5: Stereo image of a dimer step in an RNA:2′,5′-RNA helix arrangement. The sugars in the 2′,5′-RNA strand (right) adopt primarily the C2′-endo pucker, whereas those in the normal RNA strand (left) adopt the C3′-endo conformation.

Table 2: Comparative Geometry and Computed Energy of Duplexes Shown in Figure 4

duplex[a]	helix type	sugar pucker[b]	P−P distance (minor groove)[c]	av energy/bp[d]
DNA:DNA	B	D_S:D_S	18.4	2.0
RNA:RNA	A	R_N:R_N	17.9	0.0
RNA:DNA	A-like	R_N:$D_{S>N}$	18.0	3.3
RNA:2′,5′-RNA	A-like	R_N:2′5′-$R_{S>N}$	17.0	5.0
DNA:2′,5′-RNA	A-like	2′,5′-$R_{S>N}$:D_S	17.0	8.4

[a] DNA/DNA: = 5′-GTT ACC AGA-3′/3′-CAA TGG TCT-5′ (9-bp duplex); RNA:RNA, RNA:2′,5′-RNA, and RNA:DNA have the same sequence as DNA:DNA. [b] D = DNA; R = RNA; S = C2′-endo; N = C3′-endo. [c] Average interstrand phosphorus−phosphorus distance in angstroms (minor groove). [d] Average relative energies (in kilocalories per mole) computed with respect to the lowest energy RNA:RNA duplex taken as zero.

linked oligonucleotides (e.g., 2′,5′-DNA and 2′,5′-RNA) more readily bind to single-stranded RNA over single-stranded DNA (*6*, *8*, *46*). Apart from 2′,5′-linked systems, only very few oligonucleotide analogues exist that can discriminate between DNA and RNA, and these systems are very different from the natural structures (*46*, *47* and references therein). DNA is known to be more flexible than RNA, which fact manifests itself in that double helices of the latter usually form A-type helices, whereas duplex DNA is polymorphic (*28*). Thus, from this perspective, one would expect that any modified oligomer that binds to RNA should also complex ssDNA.

The ribose 2′-hydroxyl group, a chemical moiety that distinguishes RNA from DNA, is known to play a key role in the stabilization of RNA tertiary structure (*48*). Hence, one may be tempted to speculate that the enhanced stability of RNA:[2′,5′-oligomer] duplex relative to DNA:[2′,5′-oligomer] is due to interactions involving the RNA 2′-hydroxyl groups. Another contributing factor could be the preorganization of a 2′,5′-linked strand; e.g., the C3′-endo form of 2′,5′-DNA strands would better fit the A-form helical structure (*46*, *49*). A related phenomenon is the striking stability of A-type duplexes formed between 3′,5′-linked 2′-OMe RNA and complementary RNA (*50*, *51*).

Matteucci and coworkers have stated that through the model-building study of RNA:2′,5′-thioformacetal-DNA duplexes, "in canonical A and B form helices, the 2′,5′-connection is pushed into the minor groove relative to the 3′,5′-connection. The phosphodiester linkage, therefore, would be tolerated more in the wide minor groove of A helix, relative to the narrow minor groove of B form helix" (*8*). A similar conclusion was reached by Switzer and coworkers through NMR and molecular modeling studies of pure 2′,5′-DNA:2′,5′-DNA duplexes (*45*). Finally, Switzer (*6*) and Damha (*46*) have proposed that the absence of complexation

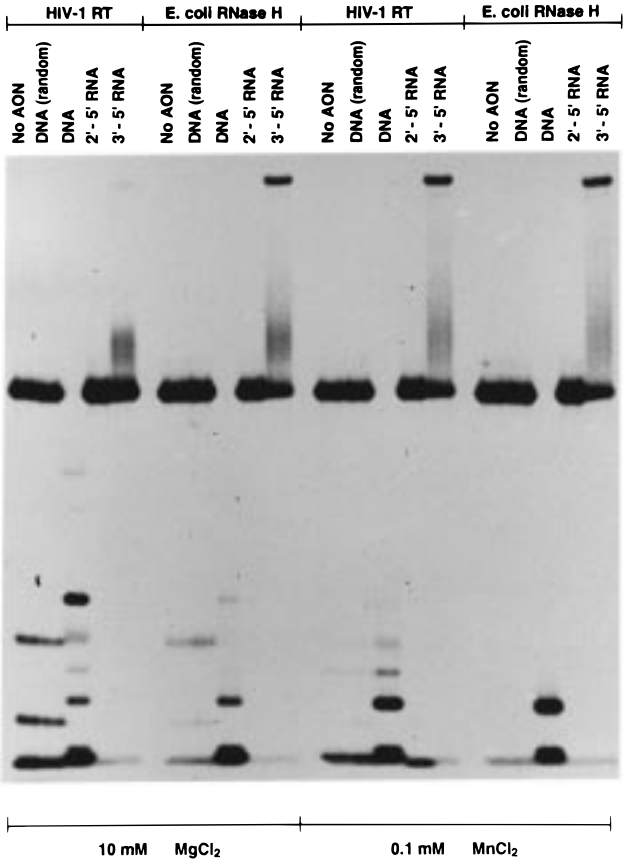

FIGURE 6: Ribonuclease H degradation of various 18-bp oligonucleotide hybrid duplexes. A 18-nt 5′-^{32}P-labeled 3′,5′-RNA was preannealed with exactly complementary 18-nt DNA, RNA, or 2′,5′-RNA oligonucleotides and then added to reaction assays containing either HIV-1 RT or *E. coli* RNase H at the indicated divalent cationic metal concentrations. Base sequences of duplexes are given in Table 1 (R region). The slowly migrating band in the 3′,5′-RNA lanes is the RNA:RNA duplex (T_m 85 °C) which withstands the denaturing conditions of the gel electrophoresis and the heating of the sample to 100 °C prior to being loaded onto the gel. See Materials and Methods for experimental conditions.

between 2′,5′-linked oligomers and natural DNA in solution may be due to the reluctance of natural DNA strands to assume a *pure* A-form conformation (C3′-endo pucker), or that the 2′,5′-isomeric strands are unable to force the DNA complement into an A-type helical structure. Although it was possible to construct a DNA:2′,5′-RNA duplex having an A-type structure (Figure 4), this was predicted to be the least stable among all duplex combinations, which is in accord with our experimental observations (refs *2* and *3*; Table 2). On the basis of the presently available data, we cannot decide which of the above effects is more important, but we suspect that more than one of these is operating in a crucial way. Clearly, high-field NMR analysis and crystal-

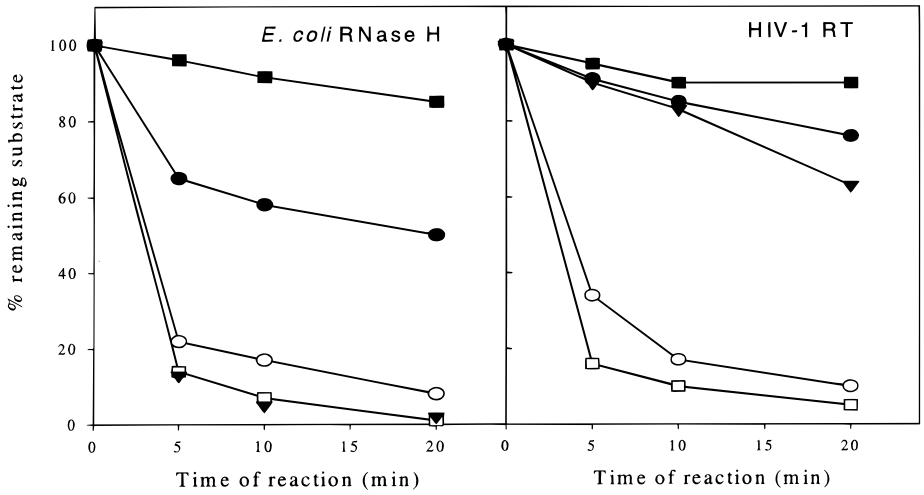

FIGURE 7: Inhibition of in vitro RNase H activity by various oligonucleotide duplexes. The experiments measured the time-dependent decrease in the amount of the 23-nt RNA component of a 5′-^{32}P-labeled RNA:DNA duplex substrate, in the absence (□) or the presence of a 2.5-fold excess of unlabeled RNA:DNA (▼), RNA:RNA (■), DNA:DNA (○), or RNA:2′,5′-RNA (●). Experimental details are provided in Materials and Methods.

lographic work on RNA:2′,5′-RNA duplexes are needed to gain understanding of this unusual RNA selectivity.

RNase H Induction Assays. RNase H is an enzyme that hydrolyzes the RNA strand of an RNA:DNA duplex, and its activity has been implicated in the antisense mechanism of oligodeoxyribonucleotides (*52*). Although RNase H cleaves only the RNA strand of the hybrid, this action is very much dependent on the nature of the antisense component. For example, *E. coli* RNase H binds duplex RNA but cannot cleave it (*53, 54*). Similarly, RNA:[antisense] hybrids in which the antisense strand is methylphosphonate DNA, α-glycoside DNA, and 2′-OMe RNA are not substrates for RNase H, whereas RNA:[phosphorothioate DNA] and RNA:[dithioate DNA] hybrids evoke RNase H activity (*1*). Lima and Crooke have also observed that binding specificity is dependent on helical conformation, with better binding affinity exhibited for A-form-like helices (duplex RNA) than for B-form helices (duplex DNA) (*54*).

The similarity of the structure of RNA:2′,5′-RNA to that of the natural RNA:DNA substrate prompted us to examine whether the RNA:2′,5′-RNA duplex would serve as a substrate for RNase H. As controls, we also examined the ability of RNA:DNA and RNA:RNA duplexes of the same sequence to serve as substrates for RNase H. As seen in Figure 6, both *E. coli* RNase H and HIV-1 RT-associated RNase H were only able to degrade RNA in the RNA:DNA hybrid; neither the RNA:2′,5′-RNA heteroduplex nor the RNA:RNA duplex served as a substrate for RNase H (Mg^{2+} or Mn^{2+} as cofactor).

The lack of activity of RNase H with the RNA:2′,5′-RNA duplex could be due to the inability of the enzyme to use the duplex as a substrate or alternatively to the inability of the RNA:2′,5′-RNA duplex to bind to the RNase H active site. To assess the latter possibility, we carried out competition binding studies in which we examined the ability of the various duplexes to inhibit RNase H degradation of a 5′-^{32}P-labeled RNA:DNA duplex substrate (Figure 7). Under our experimental conditions, in the absence of added competitor duplex, the 5′-^{32}P-labeled substrate was rapidly degraded both by HIV-1 RT RNase H ($k = 0.15$ min^{-1}) and *E. coli* RNase H ($k = 0.2$ min^{-1}). Degradation of the 5′-^{32}P-labeled 3′,5′-RNA:DNA duplex substrate by HIV-1 RT RNase H was significantly reduced by the addition of an excess of unlabeled RNA:DNA duplex competitor ($k = 0.014$ min^{-1}); similar decreases were noted in reactions containing the RNA:2′,5′-RNA and the RNA:RNA duplexes (Figure 7), implying that these complexes were indeed able to bind to the RNase H domain of HIV-1 RT. No inhibition was noted in reactions containing the DNA:DNA duplex. Interestingly, degradation of the 5′-^{32}P-labeled RNA:DNA duplex substrate by *E. coli* RNase H was not altered by the addition of an excess of unlabeled RNA:DNA duplex competitor. This was not the case for HIV-1 RT RNase H, implying that the *E. coli* enzyme has a higher capacity for degrading the RNA component of a RNA:DNA duplex than does HIV-1 RT RNase H (Figure 7).

The RNA:2′,5′-RNA and RNA:RNA duplexes inhibited degradation of the 5′-^{32}P-labeled RNA:DNA duplex substrate by *E. coli* RNase H. As noted with HIV-1 RT, the DNA:DNA duplex did not inhibit *E. coli* RNase H activity (Figure 7). These observations are consistent with the findings of Lima and Crooke (*54*), whose studies indicate that *E. coli* RNase H binds A-form duplexes (RNA:RNA) tighter than B-form duplexes (DNA:DNA).

CONCLUSIONS

2′,5′-Linked oligoribonucleotides of mixed base composition bind selectively to complementary single-stranded RNA but not to DNA. An RNA:2′,5′-RNA duplex did not elicit RNase H activity either by HIV-1 RT or by *E. coli* ribonuclease H, despite its structural similarity to an RNA:DNA hybrid. Nonetheless, addition of RNA:2′,5′-RNA hybrids to in vitro RNase H assays resulted in substantial inhibition of activity against the normal RNA:DNA duplex substrate. These properties raise the possibility of the utility of 2′,5′-RNA (and their analogues) in antiretroviral applications. For example, the selectivity of 2′,5′-RNA for interaction with RNA rather than DNA strands suggests that 2′,5′-RNA might be useful for targeting retroviral genomic RNA to inhibit early stages of reverse transcription. In addition, hairpins "aptmers" designed with the proper combination of

2′,5′-RNA and (complementary) RNA segments may inhibit the removal of the RNA component of the RNA:DNA hybrid formed during reverse transcription. RNA:2′,5′-RNA aptmers may also be serve as probes for distinguishing between RNase H-induced and hybridization arrest (translation arrest) antisense activity.

REFERENCES

1. Crooke, S. T., and Lebleu, B. (1993) *Antisense Research and Applications*; p 579, CRC Press, Boca Raton, FL.
2. Damha, M. J., Giannaris, P. A., and Khan, N. (1991) *Nucleic Acids Res. Symp. Ser. 24*, 290.
3. Giannaris, P. A., and Damha, M. J. (1993) *Nucleic Acids Res. 20*, 4742−4749.
4. Alul, R., and Hoke, G. D. (1995) *Antisense Res. Dev. 5*, 3−11.
5. Sheppard, T. L., and Breslow, R. C. (1996) *J. Am. Chem. Soc. 118*, 9810−9811.
6. Prakash, T. P., Jung, K.-E., and Switzer, C. (1996) *Chem. Commun.*, 1793−1794.
7. Bhan, P., Bhan, A., Hong, M., Hartwell, J. G., Saunders, J. M., and Hoke, G. D. (1997) *Nucleic Acids Res. 25*, 3310−3317.
8. Pudlo, J. S., Cao, X., Swaminathan, S., and Matteucci, M. D. (1994) *Tetrahedron Lett. 35*, 9315−9318.
9. Kandimalia, E. R., Manning, A., Zhao, Q., Shaw, D. R., Byrn, R. A., Sasisekharan, V., and Agrawal, S. (1997) *Nucleic Acids Res. 25*, 370−378.
10. Xiao, W., Li, G., Maitra, R. K., Maran, A., Silverman, R. H., and Torrence, P. F. (1997) *J. Med. Chem. 40*, 1195−1200.
11. Gu, Z., Fletcher, R. S., Arts, E. J., Wainberg, M. A., and Parniak, M. A. (1994) *J. Biol. Chem., 269*, 28118−28122.
12. Fletcher, R. S., Holleschak, G., Nagy, E., Arion, D., Borkow, G., Gu, Z., Wainberg, M. A., and Parniak, M. A. (1996) *Protein Expression Purif. 7*, 27−32.
13. Arts, E. J., Li, X., Gu, Z., Kleiman, L., Parniak, M. A., and Wainberg, M. A. (1994) *J. Biol. Chem. 269*, 14672−14680.
14. Wu, T., and Ogilvie, K. K. (1990) *J. Org. Chem. 55*, 4717−4724.
15. Damha, M. J., and Ogilvie, K. K. (1993) in *Methods in Molecular Biology, Volume 20, Protocols for Oligonucleotides and Analogues: Synthesis and Properties* (Agrawal, S., Ed.) pp 81−114, The Humana Press, Inc. Totowa, NJ.
16. Wasner, M. (1995) Ph.D. Thesis, Konstanz University.
17. Sproat, B., Colonna, F., Mullah, B., Tsou, D., Andrus, A., Hampel, A., and Vinayak, R. (1995) *Nucleosides Nucleotides 14*, 255−273.
18. Wincott, F., DiRenzo, A., Shaffer, C., Grimm, S., Tracz, D., Workaman, C., Sweedler, D., Gonzalez, C., Scaringe, S., and Usman, N. (1997) *Nucleic Acids Res. 23*, 2677−2684.
19. Gasparutto, D., Livache, T., Bazin, H., Duplaa, A.-M., Guy, A., Khorlin, A., Molko, D., Roget, A., and Teoule, R. (1992) *Nucleic Acids Res. 20*, 5159−5166.
20. Puglisi, J. D., and Tinoco, I., Jr. (1989) *Methods in Enzymology* (Dahlberg, J. E., and Abelson, J. N., Eds.) Vol. 180, pp 304−325, Academic Press, Inc., San Diego.
21. Alberts, B. (1989) *Molecular Biology of the Cell*, p 304, Garland Publishing, Inc., New York.
22. Borkow, G., Arion, D., Noronha, A., Scartozzi, M., Damha, M. J., and Parniak, M. A. (1997) *Int. J. Biochem. Cell Biol. 29*, 1285−1295.
23. Usman, N., Ogilvie, K. K., Jiang, M.-Y., and Cedergren, R. J. (1987) *J. Am. Chem. Soc. 109*, 7845−7854.
24. Kierzek, R., Liyan, H., and Turner, D. H. (1992) *Nucleic Acids Res. 20*, 1685−1690.
25. Hashimoto, H., and Switzer, C. (1992) *J. Am. Chem. Soc. 114*, 6255−6256.
26. Dougherty, J. P., Rizzo, C. J., and Breslow, R. (1992) *J. Am. Chem. Soc. 114*, 6254−6255.
27. Jung, K.-E., and Switzer, C. (1994) *J. Am. Chem. Soc. 116*, 6059−6061.
28. Saenger, W. (1984) *Principles of Nucleic Acids Structure* (Cantor, C. R., Ed.) Springer Verlag, New York.
29. Ojha, R., Dhingra, M., Sarma, M., Myer, Y. P., Setlik, R., Shibata, M., Kazim, A., Ornstein, R. L., Rein, R., Turner, C. J., and Sarma, R. H. (1997) *J. Biomol. Struct. Dyn. 15*, 185−215.
30. Wang, A. C., Kim, S. G., Flynn, P. F., Chou, S.-H., Orban, J., and Reid, B. R. (1992) *Biochemistry 31*, 3940−3946.
31. Ratmeyer, L., Vinayak, R., Zhong, Y. Y., Zon, G., and Wilson, W. D. (1994) *Biochemistry 33*, 5298−5304.
32. Hung, S.-H., Yu, Q., Gray, D. M., and Ratliff, R. L. (1994) *Nucleic Acids Res. 22*, 4326−4334.
33. Clark, C. L., Cecil, P. K., Singh, D., and Gray, D. M. (1997) *Nucleic Acids Res. 25*, 4098−4105.
34. Salazar, M., Champoux, J. J., and Reid, B. R. (1993) *Biochemistry 32*, 739−744.
35. Salazar, M., Federoff, O. Y., and Reid, B. R. (1996) *Biochemistry 35*, 8126−8135.
36. Ts'o, P. O. P., Kondo, N. S., Schwizer, M. P., and Hollis, D. P. (1969) *Biochemistry 8*, 997−1029.
37. Kondo, N. S., Holmes, H. M., Stempel, L. M., and Ts'o, P. O. P. (1970) *Biochemistry 9*, 3479−3499.
38. Brahms, J., Maurizot, J., and Michelson, A. M. (1967) *J. Mol. Biol. 25*, 481−495.
39. Sussman, J. L., Barzilya, I., Keren-Zur, M., and Lapidot, Y. (1973) *Biochim. Biophys. Acta 308*, 189−197.
40. Doornbos, J., Den Hartog, J. A. J., van Boom, J. H., and Altona, C. (1981) *Eur. J. Biochem. 116*, 403−412.
41. Damha, M. J., and Ogilvie, K. K. (1988) *Biochemistry 27*, 6403−6416.
42. Lalitha, V., and Yathindra, N. (1995) *Curr. Sci. 68*, 68−75.
43. Wodak, S. Y., Liu, M. Y., and Wyckoff, H. W. (1977) *J. Mol. Biol. 116*, 855−875.
44. Krishnan, R., Seshadri, T. P., and Viswamitra, M. A. (1991) *Nucleic Acids Res. 19*, 379−384.
45. Robinson, H., Jung, K.-E., Switzer, C., and Wang, A. H.-J. (1995) *J. Am. Chem. Soc. 117*, 837−838.
46. Damha, M. J., Meng, B., Wang, D., Yannopoulos, C. G., and Just, G. (1995) *Nucleic Acids Res. 19*, 3967−3973.
47. Fujimoro, S., Shudo, K., and Hashimoto, Y. (1990) *J. Am. Chem. Soc. 112*, 7436−7437.
48. Berger, I., and Egli, M. (1997) *Chem. Eur. J. 3*, 1400−1404.
49. Griffey, R. H., Lesnik, E., Freir, S., Sanghvi, Y., Teng, K., Kawasaki, A., Guinosso, C., Wheeler, P., and Mohan, V. (1994) *Carbohydrate Modifications in Antisense Research* (Sanghvi, Y., and Cook, P. d., Eds.) ACS Symposium Series 580, pp 212−224, American Chemical Society, Washington, DC.
50. Inoue, H., Hayase, Y., Imura, A., Iwai, S., Miura, K., and Ohtsuka, E. (1987) *Nucleic Acids Res. 15*, 6131−6148.
51. Lesnik, E. A., Guinosso, C. J., Kawasaki, A. M., Sasmor, H., Zounes, M., Cummins, L. L., Ecker, D. J., Dan Cook, P., and Freir, S. M. (1993) *Biochemistry 32*, 7832−7838.
52. Walder, R. Y., and Walder, J. A. (1988) *Proc. Natl. Acad. Sci. U.S.A. 85*, 5011−5015.
53. Oda, Y., Iwai, S., Ohtsuka, E., Ishikawa, M., Ikehara, M., and Nakamura, H. (1993) *Nucleic Acids Res. 21*, 4690−4695.
54. Lima, W. F., and Crooke, S. T. (1997) *Biochemistry 36*, 390−398.

BI980160B